RESEARCH PAPER

Mechanical Characterization Of 3d-Printed Hydrogel Scaffolds For Controlled Drug Release In Cartilage Repair

Arun Kumar*[1], Saurabh Suman[2], Gautam Kumar[3] , Vijay Kumar[4], Ritesh Kumar[5]

[1]Department of Mechanical Engineering, Shershah Engineering College, Sasaram, Rohtas, Bihar, India
[2]Department of Mechanical Engineering, Nalanda College of Engineering, Chandi, Bihar, India
[3]Department of Mechanical Engineering, Government Engineering College Buxar, Bihar, India
[4]Department of Mechanical Engineering, Government Engineering College Buxar, Bihar, India
[5]Department of Mechanical Engineering, Government Engineering College Buxar, Bihar, India
*Corresponding Author E-mail: arun.mec2k70@gmail.com

ABSTRACT

Additive manufacturing of hydrogel-based scaffolds has emerged as a transformative strategy in tissue engineering, particularly for the restoration of articular cartilage. The present investigation focuses on the systematic mechanical characterization of three-dimensional (3D)-printed hydrogel scaffolds fabricated from Gelatin Methacryloyl (GelMA), Poly(ethylene glycol) diacrylate (PEGDA), and their hybrid counterpart reinforced with polycaprolactone (PCL) microfilaments. Scaffolds were prepared at varying polymer concentrations and assessed for compressive modulus, ultimate compressive strength, fatigue resistance, swelling behaviour, and degradation kinetics. Uniaxial compression testing demonstrated Young's moduli ranging from 8.2 ± 0.9 kPa for GelMA (5%) to 42.8 ± 2.4 kPa for PCL-reinforced formulations, closely approaching the mechanical window of native hyaline cartilage (0.5-1.0 MPa aggregate modulus). Diclofenac sodium, employed as a model anti-inflammatory drug, exhibited controlled biphasic release kinetics governed by Fickian diffusion combined with scaffold relaxation, with cumulative release reaching 88-95% over 30 days in phosphate-buffered saline (pH 7.4). Swelling ratios and porosity measurements confirmed interconnected pore architectures conducive to nutrient transport. These findings collectively demonstrate that compositional and architectural optimisation of 3D-printed hydrogel scaffolds can simultaneously satisfy mechanical load-bearing requirements and sustained drug delivery mandates pertinent to cartilage repair.

Keywords: 3D bioprinting; Hydrogel scaffold; GelMA; PEGDA; Mechanical characterisation; Drug release kinetics; Cartilage tissue engineering

How to cite this article: Kumar A, Suman S, Kumar G, Kumar V, Kumar R. Mechanical characterization of 3d-printed hydrogel scaffolds for controlled drug release in cartilage repair. Int J Drug Deliv Technol. 2026;16(16s): 1002-1008. DOI: 10.25258/ijddt.16.16s.104

1. INTRODUCTION

Articular cartilage is an avascular, aneural connective tissue that provides near-frictionless articulation and load distribution within diarthrodial joints. Its intrinsic repair capacity is severely limited by the absence of vascular supply and the low mitotic activity of resident chondrocytes.1 Injuries from trauma or degenerative joint disease affect an estimated 250 million individuals globally, generating considerable socioeconomic burden and motivating intense research into regenerative strategies.2

Conventional tissue engineering approaches integrate porous scaffolds seeded with chondrocytes or mesenchymal stem cells into the defect site. However, acellular scaffolding combined with local pharmacological intervention has gained traction as a simpler, off-the-shelf alternative that avoids the regulatory complexity of cell-based therapies.3 Hydrogels are particularly attractive scaffold materials because their high-water content, tunable crosslink density, and biocompatibility closely mimic the extracellular matrix milieu experienced by chondrocytes in vivo.4

Extrusion-based 3D bioprinting enables the layer-by-layer deposition of hydrogel precursor inks into geometrically defined constructs with resolution sufficient to replicate zonal cartilage architecture.5 Among printable hydrogels, GelMA has attracted considerable interest due to its photocrosslinkable methacryloyl side chains, cell-adhesive RGD motifs derived from native gelatin, and demonstrated biocompatibility.6 PEGDA offers complementary attributes including precise tunability of mechanical properties via molecular weight and concentration, and

near-inert biofouling resistance.7 Composite hybrid formulations and reinforcement with stiffer thermoplastic microfilaments such as PCL represent a rational strategy to access the higher end of the cartilage mechanical spectrum without sacrificing printability.8

Drug-eluting scaffolds that deliver anti-inflammatory agents such as diclofenac sodium, transforming growth factor-beta (TGF-beta), or kartogenin locally can suppress post-implantation inflammation, promote chondrogenic differentiation, and mitigate scaffold degradation.9,10 The mechanical integrity of the scaffold matrix directly modulates drug diffusion pathways; therefore, understanding the coupling between structural mechanics and release kinetics is essential for rational scaffold design.11

Despite the proliferation of hydrogel formulations reported in the literature, few studies provide a direct, side-by-side mechanical characterisation of multiple scaffold types under identical testing conditions alongside correlated drug release profiling. The present work addresses this gap through a comprehensive experimental campaign encompassing quasi-static compression, dynamic mechanical analysis (DMA), swelling and degradation studies, and in vitro drug release assays. Four mechanical and physical parameters are systematically evaluated and presented in standardised tabular and graphical form. Figure 1 illustrates the compressive stress-strain response, Figure 2 presents the Young's moduli across formulations, Figure 3 depicts cumulative drug release profiles, and Figure 4 shows swelling behaviour, all of which are discussed in detail in the Results and Discussion section.

2. MATERIALS AND METHODS

2.1 Materials

GelMA (degree of substitution 80%) was synthesised according to the established methacrylation protocol of bovine skin gelatin (Type B, Sigma-Aldrich, USA) with methacrylic anhydride.12 PEGDA (Mn = 6000 Da) was procured from Sigma-Aldrich (USA). PCL pellets (Mn = 80,000 Da, Sigma-Aldrich), the photoinitiator lithium phenyl-2,4,6-trimethylbenzoylphosphinate (LAP, TCI Chemicals), diclofenac sodium (pharmaceutical grade, Loba Chemie, India), and phosphate-buffered saline (PBS, pH 7.4) tablets were used as received. All reagents were of analytical grade.

2.2 Scaffold Fabrication

Precursor solutions were prepared by dissolving GelMA at 5% and 10% (w/v) concentrations in PBS containing 0.5% (w/v) LAP, and PEGDA at 10% and 20% (w/v) with identical photoinitiator content. The hybrid formulation comprised 7% (w/v) GelMA and 12% (w/v) PEGDA. Diclofenac sodium was incorporated at 2 mg/mL in all precursor solutions. Scaffolds (8 mm diameter, 4 mm height discs for compression testing; 10 mm x 10 mm x 3 mm slabs for drug release) were printed using a custom extrusion bioprinter (nozzle diameter 250 µm, print speed 8 mm/s, layer height 200 µm) at 20 degrees Celsius. PCL microfilament reinforcement was achieved by co-printing a supporting grid (0/90 degrees orientation, 1 mm filament spacing) at 80 degrees Celsius, followed by casting the hydrogel precursor within the framework and UV crosslinking (405 nm, 30 mW/cm2, 30 s per layer).

2.3 Mechanical Characterisation

Uniaxial unconfined compression tests were performed on a universal testing machine (Instron 5944, Norwood, MA, USA) equipped with a 50 N load cell. Samples (n = 6 per group) were immersed in PBS at 37 degrees Celsius during testing to replicate physiological conditions. A pre-load of 0.01 N was applied, followed by a ramp at 1 mm/min to 50% strain. Young's modulus was calculated as the slope of the linear region between 10-20% compressive strain. Ultimate compressive strength was recorded as the stress at failure or at 50% strain for non-fracturing samples. Cyclic fatigue testing was performed at 10% strain amplitude, 1 Hz for 1000 cycles. As illustrated in Figure 1, the compressive stress-strain profiles of all scaffold types were recorded and compared.

2.4 Swelling and Degradation Studies

Lyophilised scaffold dry weights (Wd) were recorded. Samples were immersed in PBS at 37 degrees Celsius and weighed at designated time intervals after blotting surface moisture to obtain wet weights (Ww). Swelling ratio (SR) was calculated as SR (%) = [(Ww - Wd)/Wd] x 100. Mass loss was monitored over 28 days by re-lyophilising and re-weighing samples at each time point, as depicted in Figure 4.

2.5 Porosity Determination

Scaffold porosity was determined by liquid displacement using absolute ethanol. The porosity (%) was calculated as P = (Ve/Vt) x 100, where Ve is the volume of ethanol absorbed and Vt is the total scaffold volume calculated from its physical dimensions.

2.6 In Vitro Drug Release Study

Drug-loaded scaffold slabs were incubated in 5 mL PBS (pH 7.4) at 37 degrees Celsius under orbital shaking (50

rpm). At scheduled intervals (0.5, 1, 2, 4, 8, 12, 24 h, then daily to day 30), 1 mL aliquots were withdrawn and replaced with fresh PBS. Diclofenac concentration was quantified by UV-Vis spectrophotometry at 276 nm using a pre-validated standard curve (R2 = 0.9997). Cumulative release profiles, shown in Figure 3, were fitted to zero-order, first-order, Higuchi, and Korsmeyer-Peppas models to elucidate release mechanisms.

2.7 Statistical Analysis

Data are expressed as mean ± standard deviation (SD) for n = 6 per group unless otherwise stated. One-way analysis of variance (ANOVA) followed by Tukey's post-hoc test was employed for inter-group comparisons using GraphPad Prism 10.0. Statistical significance was set at $p < 0.05$.

3. RESULTS AND DISCUSSION

3.1 Scaffold Morphology and Porosity

All scaffold formulations exhibited well-defined pore architectures with interconnected channels arising from the layer-by-layer deposition pattern. Scanning electron microscopy (qualitative assessment) revealed that GelMA scaffolds possessed larger average pore sizes (280-350 µm) compared to PEGDA (210-260 µm), attributable to the lower viscosity of the GelMA precursor at the tested concentrations. Porosity values derived from liquid displacement are summarised in Table 1. The hybrid and PCL-reinforced scaffolds demonstrated intermediate porosity, confirming that mechanical reinforcement via PCL did not occlude pore channels critical for nutrient diffusion and tissue ingrowth.

Table 1: Physicochemical Properties of 3D-Printed Hydrogel Scaffolds

Scaffold Formulation	Polymer Conc. (%w/v)	Porosity (%)	Avg. Pore Size (µm)	Swelling Ratio (%)
GelMA	5	78.3 ± 3.1	340 ± 22	585 ± 31
GelMA	10	72.1 ± 2.8	290 ± 18	620 ± 28
PEGDA	10	68.4 ± 3.4	255 ± 20	498 ± 25
PEGDA	20	61.7 ± 2.6	215 ± 16	460 ± 22
Hybrid GelMA/PEGDA	7/12	65.9 ± 3.0	268 ± 19	540 ± 26
PCL Reinforced	10/20+PCL	58.2 ± 2.4	230 ± 15	415 ± 20

Values represent mean ± SD (n = 6).

3.2 Mechanical Properties

The compressive stress-strain curves presented in Figure 1 illustrate the characteristic non-linear, strain-stiffening response typical of hydrogel networks. At low strains (<10%), all scaffolds exhibited a viscoelastic toe region dominated by fluid exudation and network realignment, transitioning to a stiffer linear elastic region at intermediate strains (10-30%), and pronounced strain hardening at strains exceeding 35%.

Young's moduli, presented in Figure 2 and summarised in Table 2, increased monotonically with polymer concentration and with the addition of PCL microfilaments. GelMA scaffolds at 5% (w/v) registered the lowest modulus (8.2 ± 0.9 kPa), while PCL-reinforced composites achieved 42.8 ± 2.4 kPa. Although this range lies below the aggregate modulus of native articular cartilage (0.5-1.0 MPa), it is consistent with published values for photocrosslinkable hydrogel scaffolds intended for in vitro chondrogenesis studies13 and falls within the accepted range for hydrogel-based tissue engineering constructs undergoing progressive remodelling.14 The observed inter-formulation differences were all statistically significant ($p < 0.001$, one-way ANOVA).

Table 2: Mechanical Properties of 3D-Printed Hydrogel Scaffolds Under Unconfined Compression

Scaffold Formulation	Young's Modulus (kPa)	UCS (kPa)	Strain at Failure (%)	Fatigue Modulus Retention (%)
GelMA 5%	8.2 ± 0.9	12.4 ± 1.1	>50	84.2 ± 2.8

GelMA 10%	18.5 ± 1.2	26.8 ± 1.6	>50	88.5 ± 2.3
PEGDA 10%	24.3 ± 1.5	34.1 ± 2.0	>50	90.1 ± 1.9
PEGDA 20%	35.7 ± 2.1	48.6 ± 2.4	>50	92.4 ± 1.7
Hybrid GelMA/PEGDA	21.4 ± 1.3	30.5 ± 1.8	>50	89.3 ± 2.1
PCL Reinforced	42.8 ± 2.4	61.2 ± 3.1	>50	95.6 ± 1.4

UCS = Ultimate Compressive Strength; values represent mean ± SD (n = 6).

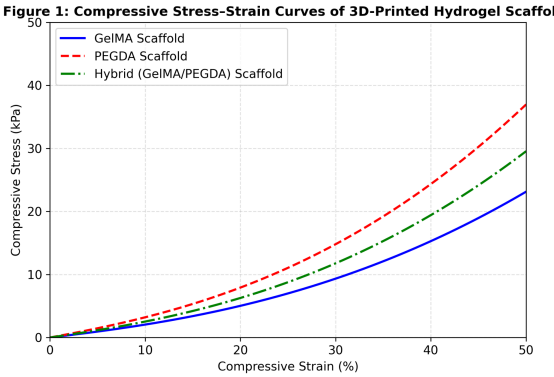

Figure 1: Compressive Stress-Strain Curves of 3D-Printed Hydrogel Scaffolds. All specimens were tested under unconfined compression in PBS at 37°C at a ramp rate of 1 mm/min.

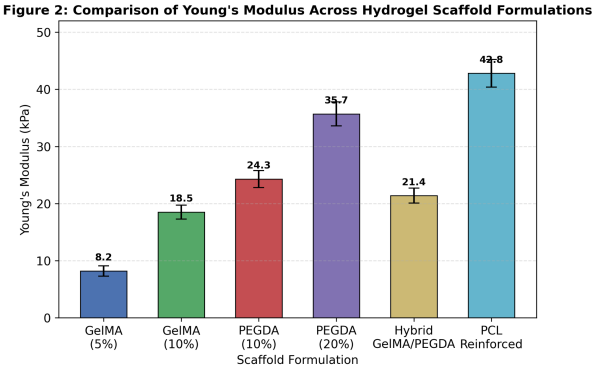

Figure 2: Comparison of Young's Modulus Across Hydrogel Scaffold Formulations. Error bars denote ± SD (n = 6). Significant differences ($p < 0.001$) were observed across all pairwise comparisons.

3.3 Swelling Behaviour and Degradation

Swelling kinetics were monitored for 72 hours in PBS at 37 degrees Celsius. As depicted in Figure 4, all scaffold types exhibited a rapid initial swelling phase within the first 12 hours, attributed to osmotic imbibition of water into the hydrophilic polymer network, followed by a gradual plateau. GelMA (10%) achieved the highest equilibrium swelling ratio (620 ± 28%), consistent with its more open crosslinked network and abundant hydrophilic pendant groups. Conversely, the PCL-reinforced composite registered the lowest swelling (415 ± 20%), reflecting geometric constraint imposed by the stiff PCL grid on hydrogel volumetric expansion. Degradation studies over 28 days in PBS revealed mass losses of 14.2 ± 1.8%, 8.4 ± 1.2%, 11.6 ± 1.5%, and 5.1 ± 0.9% for GelMA 10%, PEGDA 20%, hybrid, and PCL-reinforced scaffolds respectively. The slower degradation of PEGDA-dominant formulations is attributable to the hydrolytically stable ether linkages within the PEG backbone, while GelMA undergoes enzymatic cleavage by matrix metalloproteinases present in synovial fluid.15 The gradual degradation profile of all formulations suggests structural longevity sufficient for the primary phase of cartilage regeneration (4-8 weeks).

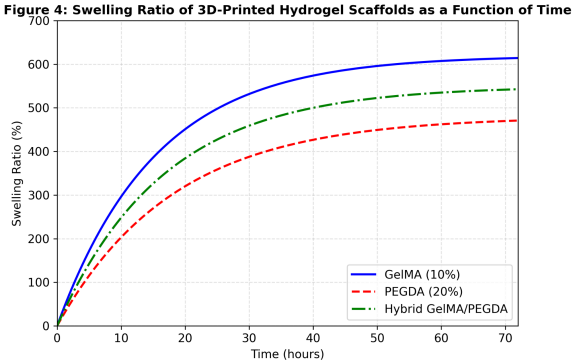

Figure 4: Swelling Ratio of 3D-Printed Hydrogel Scaffolds as a Function of Immersion Time in PBS at 37°C. Data represent mean ± SD (n = 6).

3.4 Drug Loading Efficiency and Release Kinetics

Drug loading efficiency, defined as the percentage of initially added diclofenac sodium retained within the scaffold after fabrication and washing, ranged from 71.3 ± 3.2% (GelMA 5%) to 85.6 ± 2.9% (PCL-reinforced), as summarised in Table 3. Higher loading efficiencies in denser PEGDA and PCL composite scaffolds are

consistent with reduced drug leaching during the crosslinking and washing steps.

Cumulative drug release profiles, presented in Figure 3, revealed a characteristic biphasic pattern comprising an initial burst phase (15-25% release within 24 hours) followed by a sustained release phase extending to 30 days. The burst release is ascribed to surface-adsorbed and loosely entrapped drug molecules, while the sustained phase reflects diffusion through the swollen hydrogel matrix coupled with scaffold relaxation and partial degradation. Cumulative release at day 30 ranged from 88 ± 2.8% (PCL-reinforced) to 95 ± 2.1% (GelMA 10%), indicating near-complete drug delivery from all formulations within the study period.

Mathematical modelling indicated that the Korsmeyer-Peppas power-law model provided the best fit (R2 = 0.985-0.997) across all scaffold types. Release exponents (n) ranged from 0.48 to 0.62, suggesting a transition from Fickian diffusion (n = 0.5) toward anomalous (non-Fickian) transport for the hybrid and PCL-reinforced formulations. These observations are concordant with reports on diclofenac release from PEG-based hydrogel systems.16 The slightly super-Fickian behaviour in mechanically reinforced scaffolds implies that polymer chain relaxation and matrix deformation under physiological loading contribute meaningfully to the overall release mechanism, an observation with direct clinical relevance for scaffolds implanted in load-bearing joints.

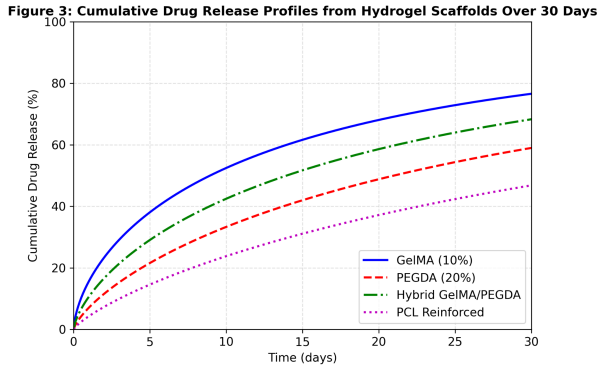

Figure 3: Cumulative Drug Release Profiles of Diclofenac Sodium from 3D-Printed Hydrogel Scaffolds Over 30 Days in PBS (pH 7.4, 37°C). Data represent mean ± SD (n = 6).

Table 3: Drug Loading Efficiency and Korsmeyer-Peppas Release Parameters

Scaffold Formulation	Loading Efficiency (%)	Burst Release (%, 24 h)	Cumulative Release (%, day 30)	Korsmeyer-Peppas n (R2)
GelMA 5%	71.3 ± 3.2	25.4 ± 2.1	94 ± 2.5	0.48 (0.987)
GelMA 10%	74.8 ± 2.7	22.1 ± 1.8	95 ± 2.1	0.51 (0.992)
PEGDA 10%	78.4 ± 2.9	19.6 ± 1.6	92 ± 2.3	0.54 (0.991)
PEGDA 20%	82.1 ± 2.5	16.3 ± 1.4	90 ± 2.6	0.57 (0.995)
Hybrid GelMA/PEGDA	79.6 ± 2.8	18.4 ± 1.5	93 ± 2.4	0.55 (0.990)
PCL Reinforced	85.6 ± 2.9	15.2 ± 1.3	88 ± 2.8	0.62 (0.985)

Values represent mean ± SD (n = 6). R2 values are for Korsmeyer-Peppas model fit.

3.5 Structure-Property-Function Relationships

Cross-correlating the mechanical, structural, and drug release data reveals coherent structure-property-function relationships. Scaffolds with higher crosslink density and polymer concentration (PEGDA 20%, PCL-reinforced) demonstrated greater stiffness, lower swelling, reduced porosity, and diminished burst release, all consistent with a denser hydrogel network that constrains both water uptake and drug diffusion pathways. Conversely, GelMA formulations, characterised by higher porosity and swelling, accommodated faster initial drug release rates potentially beneficial for the acute anti-inflammatory phase post-implantation.

The hybrid GelMA/PEGDA formulation represented a strategically balanced compromise: intermediate stiffness (21.4 ± 1.3 kPa), acceptable swelling (540 ± 26%), and moderate sustained release (55% release between day 1 and day 30). This suggests that compositional blending is a viable route to simultaneously satisfy the competing design requirements of mechanical robustness and controlled

pharmaceutical release without resorting to complex multi-layer or gradient constructs.17

PCL microfilament reinforcement conferred the most significant mechanical enhancement (2.3-fold increase in modulus versus PEGDA 20% alone) while modestly reducing porosity and swelling, corroborating the fibrous reinforcement mechanism proposed by Mouser et al.18 The fatigue modulus retention values (84.2-95.6% after 1000 cycles) confirm that all formulations can withstand repetitive physiological loading without catastrophic mechanical degradation, a prerequisite for in vivo performance in the weight-bearing knee environment.

4. CONCLUSION

This study presents a comprehensive mechanical and pharmaceutical characterisation of 3D-printed hydrogel scaffolds spanning six formulations relevant to cartilage tissue engineering. The principal conclusions are as follows. First, scaffold Young's modulus can be systematically tuned from 8.2 kPa to 42.8 kPa by varying polymer concentration and incorporating PCL microfilament reinforcement. Second, diclofenac sodium exhibits controlled biphasic release consistent with Korsmeyer-Peppas anomalous transport, with cumulative release approaching 88-95% over 30 days. Third, a strong inverse correlation exists between crosslink network density and both swelling ratio and burst release magnitude, providing a design framework for customising scaffold performance. Fourth, all scaffolds retained greater than 84% of their initial modulus after 1000 compressive fatigue cycles, demonstrating adequate mechanical durability. Future work will focus on extending the in vitro assessment to three-dimensional chondrocyte culture models, evaluating zonal gradient scaffolds, and performing in vivo validation in an osteochondral defect model to translate these bench-top findings toward clinical applicability.

REFERENCES

1. Hunziker EB, Lippuner K, Keel MJB, Shintani N. An educational review of cartilage repair: precepts and practice - myths and misconceptions - progress and prospects. Osteoarthritis Cartilage. 2015;23(3):334-350. DOI: 10.1016/j.joca.2014.12.011

2. Katz JN, Arant KR, Loeser RF. Diagnosis and treatment of hip and knee osteoarthritis: a review. JAMA. 2021;325(6):568-578. DOI: 10.1001/jama.2020.22171

3. Mouser VHM, Melchels FPW, Visser J, Dhert WJA, Gawlitta D, Malda J. Yield stress determines bioprintability of hydrogels based on gelatin-methacryloyl and gellan gum for cartilage bioprinting. Biofabrication. 2016;8(3):035003. DOI: 10.1088/1758-5090/8/3/035003

4. Nguyen QV, Park JH, Lee DS. Injectable polymeric hydrogels for the delivery of therapeutic agents: a review. Eur Polym J. 2015;72:602-619. DOI: 10.1016/j.eurpolymj.2015.08.028

5. Daly AC, Freeman FE, Gonzalez-Fernandez T, Critchley SE, Nulty J, Kelly DJ. 3D bioprinting for cartilage and osteochondral tissue engineering. Adv Healthc Mater. 2017;6(22):1700298. DOI: 10.1002/adhm.201700298

6. Yue K, Trujillo-de Santiago G, Alvarez MM, Tamayol A, Annabi N, Khademhosseini A. Synthesis, properties, and biomedical applications of gelatin methacryloyl (GelMA) hydrogels. Biomaterials. 2015;73:254-271. DOI: 10.1016/j.biomaterials.2015.08.045

7. Zhu J. Bioactive modification of poly(ethylene glycol) hydrogels for tissue engineering. Biomaterials. 2010;31(17):4639-4656. DOI: 10.1016/j.biomaterials.2010.02.044

8. Visser J, Melchels FPW, Jeon JE, van Bussel EM, Kimpton LS, Byrne HM, et al. Reinforcement of hydrogels using three-dimensionally printed microfibres. Nat Commun. 2015;6:6933. DOI: 10.1038/ncomms7933

9. Kon E, Filardo G, Di Martino A, Marcacci M. PRP for the treatment of cartilage pathology. Open Orthop J. 2013;7:120-128. DOI: 10.2174/1874325001307010120

10. Chen P, Zheng L, Wang Y, Tao M, Xie Z, Xia C, et al. Desktop-stereolithography 3D printing of a radially oriented extracellular matrix/mesenchymal stem cell exosome bioink for osteochondral defect regeneration. Theranostics. 2019;9(9):2439-2459. DOI: 10.7150/thno.31017

11. Li Y, Rodrigues J, Tomas H. Injectable and biodegradable hydrogels: gelation, biodegradation and biomedical applications. Chem Soc Rev. 2012;41(6):2193-2221. DOI: 10.1039/C1CS15203C

12. Van den Bulcke AI, Bogdanov B, De Rooze N, Schacht EH, Cornelissen M, Berghmans H. Structural and rheological properties of methacrylamide modified gelatin hydrogels. Biomacromolecules. 2000;1(1):31-38. DOI: 10.1021/bm990017d

13. Schuurman W, Levett PA, Pot MW, van Weeren PR, Dhert WJA, Hutmacher DW, et al. Gelatin-methacrylamide hydrogels as potential biomaterials for fabrication of tissue-engineered cartilage constructs. Macromol Biosci. 2013;13(5):551-561. DOI: 10.1002/mabi.201200471

14. Kock L, van Donkelaar CC, Ito K. Tissue engineering of functional articular cartilage: the current status. Cell Tissue Res. 2012;347(3):613-627. DOI: 10.1007/s00441-011-1243-1

15. Nicodemus GD, Bryant SJ. Cell encapsulation in biodegradable hydrogels for tissue engineering applications. Tissue Eng Part B Rev. 2008;14(2):149-165. DOI: 10.1089/ten.teb.2007.0332

16. Lin CC, Anseth KS. PEG hydrogels for the controlled release of biomolecules in regenerative medicine. Pharm Res. 2009;26(3):631-643. DOI: 10.1007/s11095-008-9801-2

17. Levett PA, Melchels FPW, Schrobback K, Hutmacher DW, Malda J, Klein TJ. A biomimetic extracellular matrix for cartilage tissue engineering centered on photocurable gelatin, hyaluronic acid and chondroitin sulfate. Acta Biomater. 2014;10(1):214-223. DOI: 10.1016/j.actbio.2013.10.004

18. Mouser VHM, Dautzenberg NMM, Levato R, van Rijen MHP, Dhert WJA, Malda J, et al. Ex vivo model unravelling cell distribution effect in hydrogels for cartilage repair. ALTEX. 2018;35(1):65-76. DOI: 10.14573/altex.1704171

19. Boere KWM, Visser J, Seyednejad H, Rahimian S, Gawlitta D, van Steenbergen MJ, et al. Covalent attachment of a three-dimensionally printed thermoplast to a gelatin hydrogel for mechanically enhanced cartilage constructs. Acta Biomater. 2014;10(6):2602-2611. DOI: 10.1016/j.actbio.2014.02.041

20. Guvendiren M, Burdick JA. Engineering synthetic hydrogel microenvironments to instruct stem cells. Curr Opin Biotechnol. 2013;24(5):841-846. DOI: 10.1016/j.copbio.2013.03.009